Development of Realistic Simulation Techniques to Predict Cure-Induced Microcracking in 3D Woven Composites

Harun Bayraktar[1], Igor Tsukrov[2], Michael Giovinazzo[2], Jon Goering[1], Todd Gross[2], Monica Fruscello[1], Lars Martinsson[3]

[1] Albany Engineered Composites, Rochester, NH, USA

[2] Department of Mechanical Engineering, University of New Hampshire, Durham, NH, USA

[3] Albany International, Halmstad, Sweden

Abstract: Three-dimensional woven composites that are becoming increasingly popular in aerospace applications have superior through-the-thickness strength, stiffness, and thermal conductivity compared to conventional 2D laminated composites. However, despite their advantages, many details regarding the mechanical behavior of 3D woven composites are not as well-known as they are for traditional laminated composites. Microcracking of carbon-epoxy composites during resin curing is one important example. The main goal of this study is to improve the understanding of cure-induced microcracking through the development of realistic numerical models validated with experimental data. Specifically, microcracking predictions of unit cell FEA models of two different fiber architectures are compared with results of micro-computed tomography scans of actual panels with the same fiber architectures. Abaqus/CAE is used in the model creation process and the curing process is simulated using thermal stress analysis in Abaqus/Standard. Numerical predictions of the stress concentration areas correlate well with the observations of microcracking obtained by micro-computed tomography. Significant performance gains were obtained by using the iterative equation solver.

Keywords: Aerospace, 3D Woven Composites, Microcracking, Thermal Stress, Micro-computed tomography.

1. Introduction

Composites in general are becoming increasingly common in aerospace applications due to their light weight and custom tailored properties (Figure 1). While traditional laminated composites constitute the vast majority of applications, 3D woven composites have certain advantages over laminates because the amount of fiber in all three directions can be controlled; thereby enabling the designer to tailor the stiffness and strength of the final component to the exact specifications required for successful performance. 3D woven composites have superior through-the-thickness strength, stiffness, and thermal conductivity compared to conventional 2D laminated composites. In addition, the interlocking nature of the 3D woven fiber preform leads to superior damage tolerance and fatigue behavior. However, certain weave architectures and resin systems exhibit

cure-induced microcracking in matrix pockets (Figure 2) which is not observed with 2D laminates. Presumably, the through-the-thickness constraint from the 3D weave increases the magnitude of triaxial stresses induced by curing shrinkage and the difference in the coefficient of thermal expansion (CTE) between the resin and the fibers as the composite structure cools from the resin curing temperature. While cure-induced microcracking can be eliminated by using toughened resins, it is desirable to better understand this phenomenon and to develop tools for designing microcracking resistant fiber architectures that allow the use of less expensive untoughend resins.

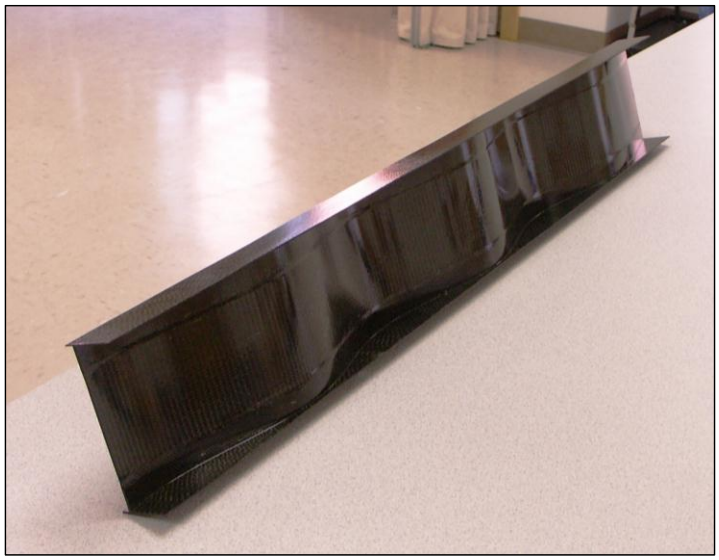

Figure 1. Sine wave beam application with 3D woven composites.

Most of the published research on 3D woven composites focuses on utilizing experimental and predictive modeling techniques to evaluate the overall stiffness of the composite for various material designs (see, for example, the list of references in Lomov et al. 2007) and to predict their strength under applied external loading (as in Cox et al. 1994, and later works). Some significant experimental and modeling results related to the process-induced residual stresses are given in Hobbiebrunken et al. (2004, 2005) but those papers are devoted to unidirectional laminates and do not cover the three-dimensional composite architectures. Therefore, the goal of this research is to develop realistic finite element models to predict cure-induced stresses in 3D woven composites and validate their predictions using micro-computed tomography (micro-CT) scans of actual samples. The simulation results are processed to evaluate the potential of different architectures to cause microcracking.

2. Materials and Methods

2.1 3D woven composite fiber architectures

Two 3D woven composite panels (4 mm thick) with significantly different fiber architectures (i.e., the particular arrangement of reinforcement within the composite) are considered in this paper, see

Figure 3. The ply-to-ply and orthogonal weave patterns represent limiting cases of through-the-thickness reinforcement for 3D woven composites.

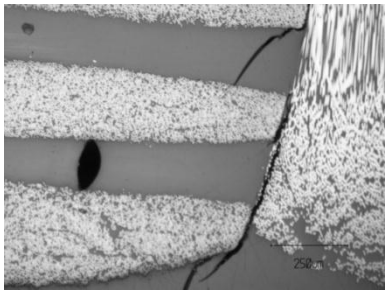

Figure 2. Example of cure-induced microcracks in the orthogonal woven composite. Carbon fibers are seen as white, resin as grey, and cracks as black objects.

The panels used in this study were manufactured by Albany Engineered Composites, Inc. (AEC) utilizing Hexcel IM7 12K carbon fiber tows and RTM6 epoxy resin. The dry preforms were woven with a computer controlled Jacquard 3D weaving loom and impregnated with resin through resin transfer molding (RTM). The panels were cured at 160ºC for 2.5 hours in the mold and then demolded and left to air-cool to room temperature.

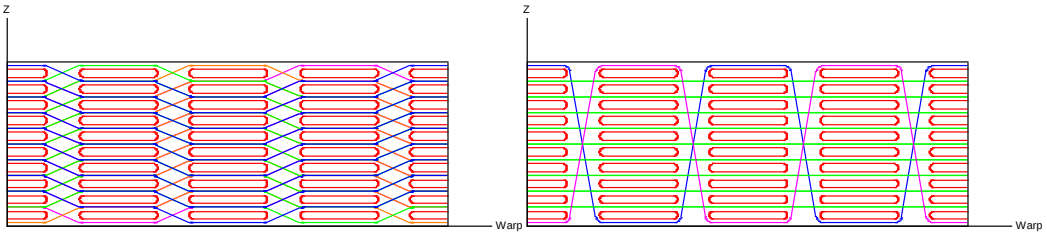

a b

Figure 3. Fiber architectures of 3D woven composites considered in this study: (a) ply-to-ply 3D weave pattern, (b) orthogonal 3D weave pattern.

Optical microscopy of the specimens shows that composites with the ply-to-ply reinforcement architecture don't develop any cure-induced microcracks. In contrast, the orthogonal weave pattern results in the formation of microcracks observed mostly in the resin pockets, but also at the interfaces and transversely through the yarns (Figure 2). It is hypothesized that for the orthogonal weave pattern, the increased level of through-the-thickness reinforcement combined with the cure shrinkage of the resin and the two orders of magnitude difference in the coefficients of thermal expansion (CTE) between the epoxy resin and carbon fiber causes microcracking. Therefore, we created realistic finite element models for each weave pattern to investigate the differences in residual stress fields that develop during the curing process.

2.2 Development of unit cell models of the composites

Thermo-mechanical behavior of woven composites can be analyzed by numerical simulations performed on the so-called unit cell (a.k.a., Representative Volume Element) of material – the smallest repeating portion of the composite, such that the entire material can be treated as an assemblage of its unit cells. The modeling procedure involves (1) development of the geometric model of the unit cell, (2) construction of the finite element mesh, (3) assignment of the mechanical properties to the finite elements including definitions of the orientations of the material symmetry axis for the transversely-isotropic tows, and (4) specification of the proper periodic boundary conditions (the periodic boundary condition formulas are given, for example, in Li 2000).

Several textile geometrical modeling software packages are available to construct a geometric model of the woven unit cell, such as TexGen (see Sherburn 2007) and WiseTex (Verpoest and Lomov 2005). They vary in how the yarn paths are defined, the cross-section definition of the tows, whether the fabric mechanics and/or composite stiffness prediction models are included, finite element meshing and compatibility with commercial FEA packages. Figure 4 presents geometric models of the unit cells developed utilizing the TexGen software package (TexGen Software Ver. 3.3.2, University of Nottingham Textile Composites Research, Nottingham, UK). While TexGen seems to be capable to model the ply-to-ply weave patterns, it cannot resolve interference (material interpenetration) between yarns in the densely packed orthogonal patterns, as shown in Figure 4c. Also, all of the above mentioned programs use an idealized tow cross-section which is defined by the modeler. However, the analysis of micrographs shows that the interaction between tows, as they are woven and processed, results in significant (and irregular) variations of their cross sections, see Figure 5c. These variations might not introduce significant changes in the overall mechanical response, but appear to be important for the modeling of local stress concentrations in the composites during curing.

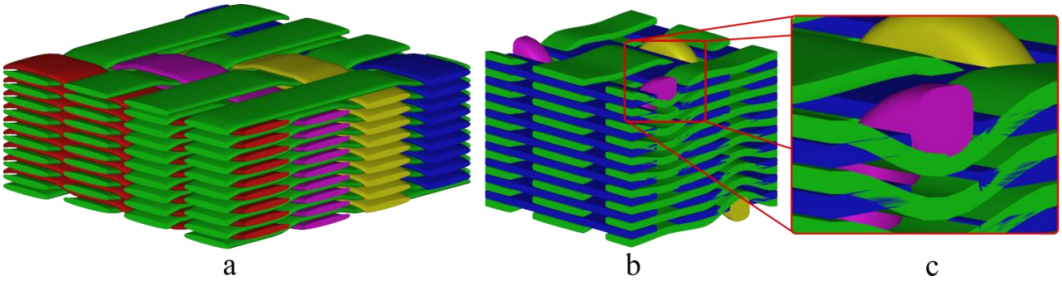

Figure 4. Preform geometry models developed in TexGen: (a) Ply-to-ply, (b) Orthogonal; (c) Interference problem in TexGen model of the orthogonal design.

To accurately capture the as-woven geometry of the considered 3D woven composites we utilize a simulation technique called the digital element method (DFMA Software Package, see Miao et al. 2008). This technique represents the tows within the composite preform as an assemblage of the adjustable number of virtual fibers modeled as a chain of truss elements. The as-woven geometry of the composite unit cell is then obtained through a series of explicit dynamic stress relaxation analyses where contact and friction interactions between tows and fibers are taken into account. We refer the reader to Miao et al. (2008) for further details. The orthogonal pattern generated

utilizing this method with 76 virtual fibers per yarn is shown in Figure 5a. The solid geometric representation of the yarns is shown in Figure 5b. When Figure 5b is compared to a cross-section micrograph of an actual sample (Figure 5c) with the same fiber architecture, the approach seems to yield very accurate results.

The as woven solid yarn geometry is imported into the commercial FEA package Abaqus/CAE (Version 6.10, Dassault Systèmes Simulia Corp., Providence, RI), where a unit cell containing this reinforcement is defined and the surrounding matrix material as well as the yarns are meshed with quadratic tetrahedral elements. The models are shown in Figure 6. The ply-to-ply architecture model has 1.09E+6 elements and 1.46E+6 nodes while the orthogonal architecture model has 5.97E+5 elements and 8.04E+5 nodes. The material properties of the isotropic resin matrix or the transversely-isotropic impregnated tows are assigned using custom software which ensures that the material orientation of each element is consistent with the fiber orientations in the as-woven model.

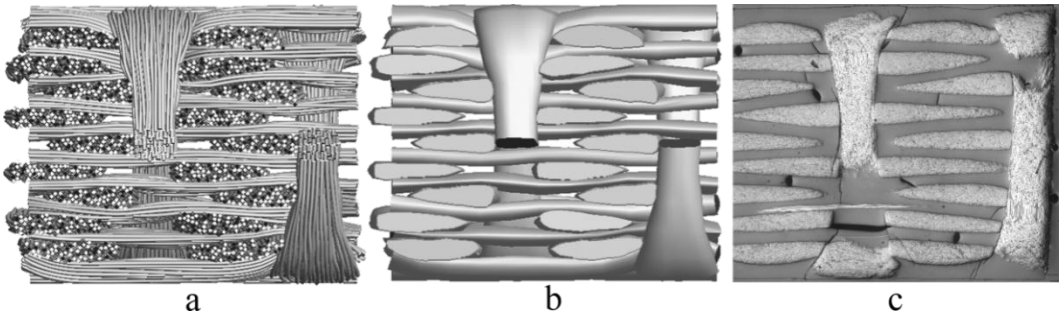

Figure 5. (a) Cross-sectional view of the orthogonal weave composite geometry obtained using the digital element method, (b) solid yarn model that can be imported to a preprocessor for meshing purposes; (c) micrograph of the actual composite.

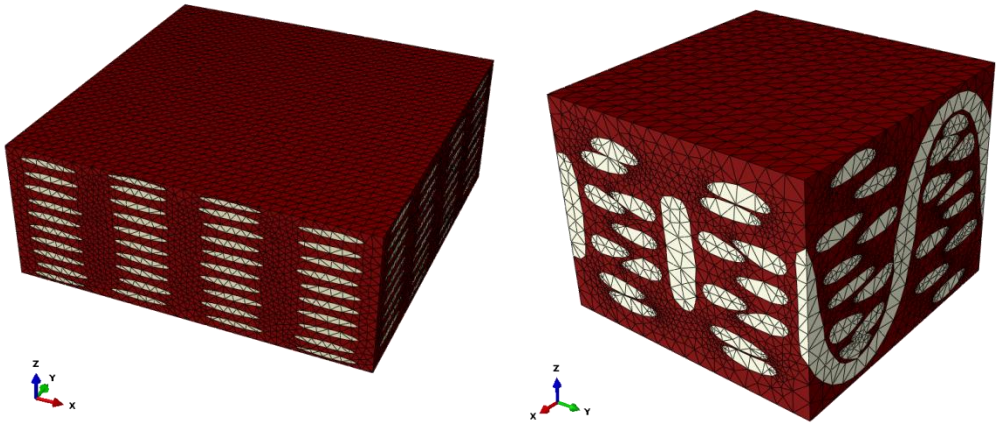

Figure 6. FEA models of 3D woven composites used in this study with ply-to-ply (left) and orthogonal architectures (right).

2.3 Homogenization of the impregnated tow properties

Impregnated tows in woven composites are traditionally treated as unidirectional bundles of fibers in a polymer matrix. The overall mechanical properties of the bundles are transversely-isotropic. Homogenization of such systems is well studied, and the numerical formulas to predict the effective elastic response are readily available. Table 1 presents the thermo-elastic properties of the constituents (fibers and matrix), and the homogenized tow properties for the volume fraction of fibers within the tow assuming $V_f = 0.8$ using the composite cylinder assemblage (CCA) model (Hashin, 1972, 1979). Direction 1 is longitudinal, and directions 2 and 3 are transverse.

Table 1. Constituent and tow properties.

Material	E_1 (MPa)	E_2 (MPa)	G_{12} (MPa)	ν_{12}	ν_{23}	α_1 (1/°C)	α_2 (1/°C)
IM7 12K Carbon Fiber	2.76E+5	2.31E+4	2.76E+4	0.35	0.30	-4.0E-7	6.0E-6
RTM6 Epoxy Resin	2.90E+3	-	-	0.30	-	6.0E-5	-
Tow	2.21E+5	1.26E+4	7.39E+3	0.34	0.32	-2.5E-7	1.7E-5

3. Results

3.1 Finite element simulations

In this section, we model process-induced stresses caused by the uniform temperature drop from the resin curing temperature to room temperature. For such simplified analysis, the matrix is treated as an isotropic linearly elastic material with a temperature-independent Young's modulus, Poisson's ratio and thermal expansion coefficient. These assumptions have to be modified for more rigorous treatment if nonlinear thermal-structural coupling and physical processes during curing are to be included in the model. However, even the linear simulations provide useful insight into relationship between weave pattern and potential microfracture of the matrix. It is assumed that the structure is subjected to a uniform temperature drop of 140°C.

Failure of polymers under triaxial loading is strongly influenced by both first and second invariants of the stress field (Asp et al, 1996). Therefore typical stress measures used for post-processing, such as von Mises stress, are not suitable for the epoxy resin. Therefore, the stress results are post-processed through a custom Python script using the Abaqus output database API. We utilize the so-called parabolic failure criterion suggested, for example, by Hobbiebrunken et al. (2004):

$$\sigma_{VM}^2 + A\sigma_H = \sigma_Y^2 \qquad (1)$$

where σ_{VM} is the equivalent (von Mises) deviatoric stress, σ_H is the hydrostatic stress, and A and σ_Y are the material constants found from tests on the neat resin. In Hobbiebrunken et al. (2004), these constants were determined for numerical modeling of unidirectional carbon/epoxy composites from uniaxial tensile and torsion tests. Note that more comprehensive studies are

needed to identify these constants for triaxial tensile stress states relevant for curing of 3D woven composites. The equivalent parabolic stress can be introduced as

$$\sigma_{PAR} = \begin{cases} \sqrt{\sigma_{VM}^2 + A\sigma_H} \text{ if } (\sigma_{VM}^2 + A\sigma_H) \geq 0 \\ -\sqrt{\sigma_{VM}^2 + A\sigma_H} \text{ if } (\sigma_{VM}^2 + A\sigma_H) < 0 \end{cases}. \quad (2)$$

This stress is calculated for all matrix elements. If its value exceeds σ_Y the material of the matrix can be expected to fail.

Figure 7 provides cumulative volume distribution of the parabolic stress in the resin for two considered reinforcement architectures after a temperature drop of 140ºC. The curve for each material shows the percentage of matrix volume with σ_{PAR} lower than the value indicated at the abscissa axis. It can be seen that if we consider a value of the parabolic stress not exceeded by 99% of the matrix in ply-to-ply architecture (σ_{PAR} = 108 MPa), about 38% of the matrix in the orthogonal architecture will have residual stresses higher than such value. Thus, the orthogonal weave architecture has significantly higher potential to produce microcracking during curing. Note that we utilized the cumulative volume distribution approach instead of analyzing the highest stresses in some particular points because interfaces with sharp corners between phases produce singularities in the linear analysis—these singularities would be observed in all weave architectures and could not help with identifying the weave patterns more likely to cause matrix damage during curing.

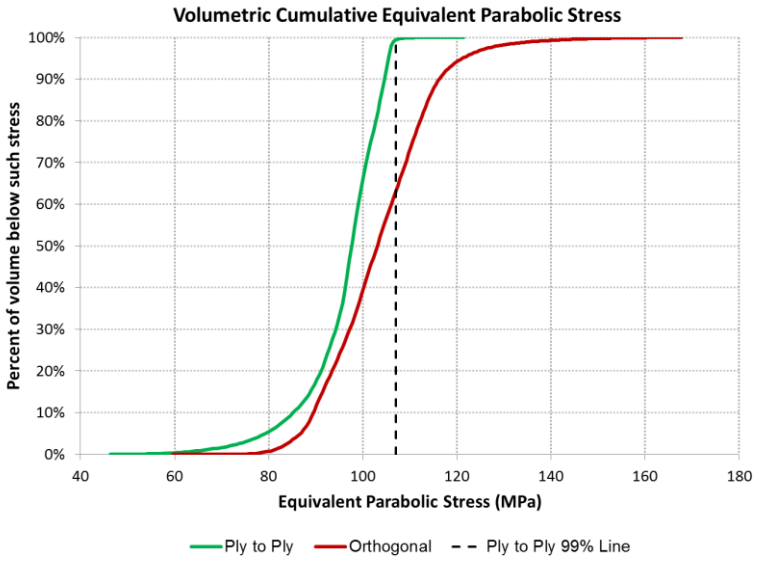

Figure 7. Cumulative volume distribution of the parabolic stress in the matrix for two different composites.

3.2 Comparison of FEA simulations with micro-CT

In order to investigate the microcracking within our 3D woven composite panels, micro-computed tomography (micro-CT) scanning on samples of both panels was performed on a SkyScan 1172 (Kontich, Belgium) system. The sample dimensions and scan resolution were chosen to ensure at least one full unit cell is scanned. This resulted in sample dimensions of 10mm x 10mm and a scan resolution of 8.2 microns. This scan resolution was adequate enough to detect microcracks within the composite samples (see discussion in Schilling et al., 2005). While no microcracks were observed in the ply-to-ply architecture, as expected from the previous optical microscopy results, many microcracks were observed in the orthogonal architecture panel. The 3D nature of the micro-CT scans makes it possible to compare the locations of microcracking with the areas of high concentration of parabolic stress in the resin matrix of the FE model.

Figure 8 provides an example of distributions of the equivalent von Mises and parabolic stresses (σ_{PAR}) in one of the cross-sections of the composite, and the micro-CT images of the corresponding area. It can be seen that location of microcracks correlates well with numerically predicted areas of concentrations of equivalent parabolic stress. There is no immediate correlation between the micro-CT observed microcracking and the areas of the elevated von Mises stress. This highlights the importance of using a stress measure suitable for the epoxy resin, which takes the hydrostatic stress into account. Results similar to the ones shown in Figure 8 were observed for other cross-sections of this orthogonally reinforced composite specimen.

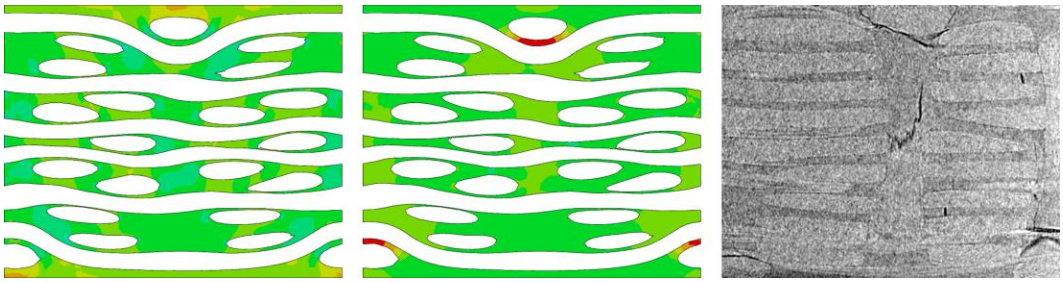

a b c

Figure 8. FEA-predicted distribution of (a) von Mises and (b) equivalent parabolic stress (σ_{PAR}). (c) Micro-CT image of the same cross-section: lighter grey –tows, darker grey – matrix, black – microcracks.

3.3 Performance gains from use of the iterative solver.

Due to the blocky topology of the microstructural unit-cell models used in this study that are moderate in size (2.4 and 4.4M dof), the number of FLOPS required by the direct solver are quite large (9.1E+13 and 2.9E+14). Therefore these models are good candidates for iterative solvers and as expected significant performance gains were obtained (Table 2) by using the iterative solver in Abaqus/Standard for the thermal stress analyses. All runs were performed on a Linux workstation with Intel X5667 processors and 24GB physical memory.

Table 2. Direct and iterative solver performance comparison.

Model	Total Simulation Wall Clock Time (s)		Speed-up
	Direct Sparse Solver (cpus=2)	Iterative Solver (cpus=1)	
Ply-to-ply (4.4M dof)	17118	3274	5.2
Orthogonal (2.4M dof)	4730	1214	3.9

4. Conclusions

Accurate finite element models are important to predict cure-induced microcracking of resin in 3D woven composites. The modeling effort presented in this paper shows that:

- It is possible to utilize numerical simulations to create models that realistically reproduce the as-woven geometry of 3D woven composites.
- In 3D woven composites, the orthogonal weave architecture produces more extensive areas of elevated parabolic stress than the ply-to-ply one due to its increased level of through-the-thickness reinforcement.
- Good agreement between FEA-simulated and micro-CT observed areas of microcracking suggests that equivalent parabolic stress can serve as an adequate measure to predict failure of epoxy resin during curing of 3D woven composites.

5. Acknowledgements

The authors gratefully acknowledge financial support of the National Science Foundation through the grant CMMI-1100409. This collaborative research was also supported by Albany Engineered Composites, Inc. and the New Hampshire Innovation Research Center.

6. References

Asp, L.E. Berglund, L.A., Talreja, R. (1996) A Criterion for Crack Initiation in Glassy Polymers Subjected to a Composite-like Stress State. Composites Science and Technology, 56, pp. 1291-1301

Cox, B. N., Dadkhah, M. S., Morris, W. L. and Flintoff, J. G. (1994). Failure mechanisms of 3D woven composites in tension, compression, and bending. Acta Metallurgica et Marerialia, 42(12), 3967-3984.

Hashin Z. (1972). Theory of Fiber-Reinforced Materials. Final Report, contract NAS1-8818, NASA CR1974, USA.

Hashin, Z. (1979). Analysis of Properties of Fiber Composites with Anisotropic Constituents. Journal of Applied Mechanics, 46, pp. 543-550.

Hobbiebrunken, T., Hojo, M., Fiedler, B., Tanaka, M., Ochiai, Sh., Schulte, K. (2004). Thermomechanical Analysis of Micromechanical Formation of Residual Stresses and Initial Matrix Failure in CFRP, JSME International Journal Series A, 47(3), pp. 349-356.

Hobbiebrunken, T., Fiedler, B., Hojo, M., Ochiai, S., Schulte, K. (2005). Microscopic yielding of CF/epoxy composites and the effect on the formation of thermal residual stresses. Composites Science and Technology, 65, pp. 1626-1635.

Li, S. (2000). General unit cells for micromechanical analyses of unidirectional composites. Composites: Part A, 32, pp. 815-826.

Lomov, S. V., Ivanov, D. S., Verpoest, I., Zako, M., Kurashiki, T., Nakai, H., Hirosawa, S. (2007). Meso-FE modelling of textile composites: Road map, data flow and algorithms. Composites Science and Technology, 67, pp. 1870-1891.

Miao, Y. Eric Zhou, Youqi Wang, and Cheeseman, B. (2008). Mechanics of textile composites: Micro-geometry. Composites Science and Technology, 68, pp. 1671-1678.

Schilling, P. J., Karedla, B. R., Tatiparthi, A. K., Verges, M. A., Herrington, P. D. (2005) X-ray computed microtomography of internal damage in fiber reinforced polymer matrix composites. Composites Science and Technology, 65, pp. 2071-2078

Sherburn, M. (2007). Geometric and mechanical modelling of textiles. Ph.D. Thesis, University of Nottingham, UK.

Verpoest I., Lomov S.V. (2005) Virtual textile composites software WiseTex: Integration with micro-mechanical, permeability and structural analysis. Composites Science and Technology, 65, 2563–2574.